



Twisting Soft Robots

Written by Sina Nabiee

Twisting Soft Robots with Physical Intelligence [1]

- Some soft robots can move by harvesting energy from the environment
- few of them can autonomously navigate only by interacting with the environment and adapting to it and without human interference and external control systems. This is called physical embodied intelligence

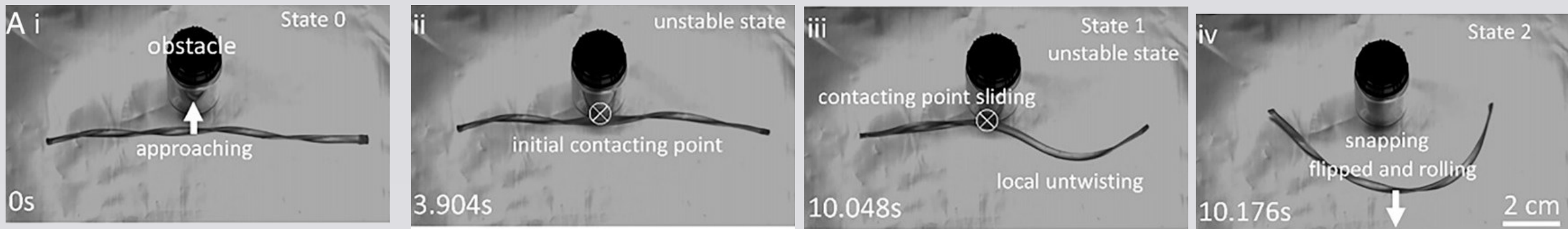


Figure 1: Twisting Soft Robot Avoiding an Obstacle



Material: Liquid Crystal elastomers (LCE) [2]

- LCEs have one of the largest reversible shape changes among solid materials making them an ideal material for soft robots, but they can also be designed to have irreversible shape changes and thus be used as shape memories.
- Soft robots made of liquid crystal elastomers can move by harnessing energy from the environment in forms of heat and light.
- Their mechanical properties and geometry change in contact with light or heat which is the reason for light based and heat based actuation

Material: Liquid Crystal elastomers (LCE) [2]

- They can form complex shapes and have oriented polymer networks or liquid crystalline phases (mesogens) that can be directed in controllable manners by actuation based on light, heat and magnetic fields.
- Adding nano materials such as Carbon nanotubes can improve the properties of LCEs especially thermal and light based actuation

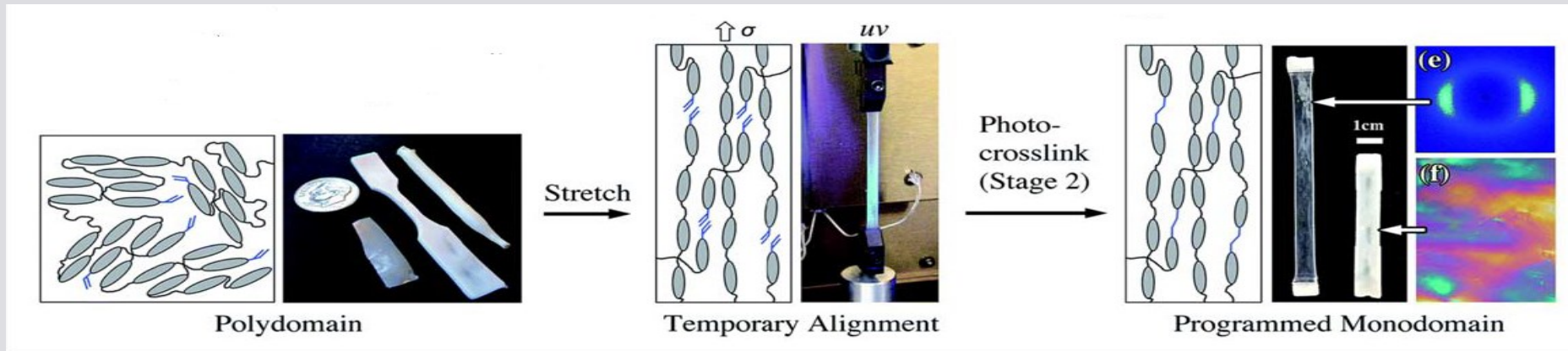
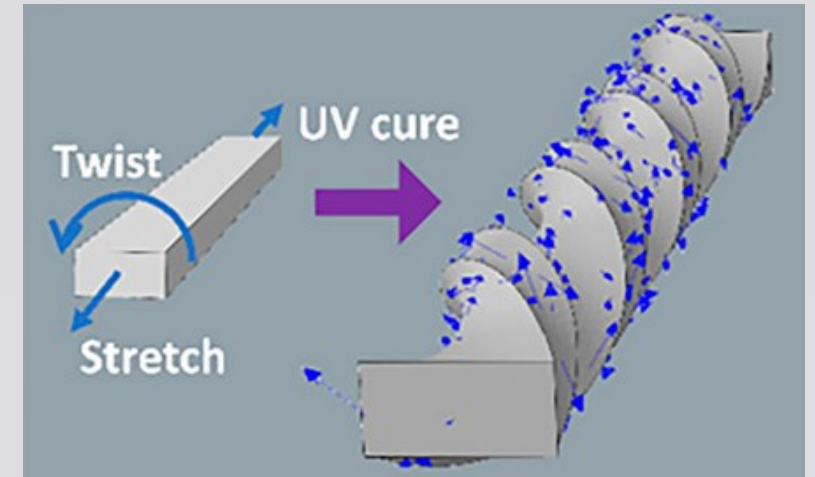


Figure 2: Polymer networks of LCEs and their alignment by mechanical and light based actuation

Manufacturing the twisting ribbon robot from LCE[1]

- Twisted LCE ribbons are simply fabricated by mechanically stretching and twisting of a rectangular flat LCE strip with its length much greater than its width and synthesized in two-stage polymerization.
- Stretching makes the mesogens aligned along with the stretching direction. When further twisted, a 3D mesogen alignment with twisted morphology is obtained

Figure 3:
Creating
Twisted
Ribbon made
of LCE





LCE Twisting Robots Dynamics[3]

- Twisted soft robots made of LCEs often have two stable states which can be switched via the process called snapping that bypasses the intermediate unstable forms.
- Snapping can be triggered by external stimuli such as mechanical forces, light and heat.
- Self sustained oscillatory snapping between the two stable states in systems with geometric asymmetries induces directional motion by creating asymmetric friction forces.

LCE Twisting Robots Dynamics[3]

- Snapping can be triggered only by external stimuli that are large enough to overcome the energy barrier and generate sufficient moments.
- Without external source of energy such as heat or light snapping oscillation exponentially decays.[4]

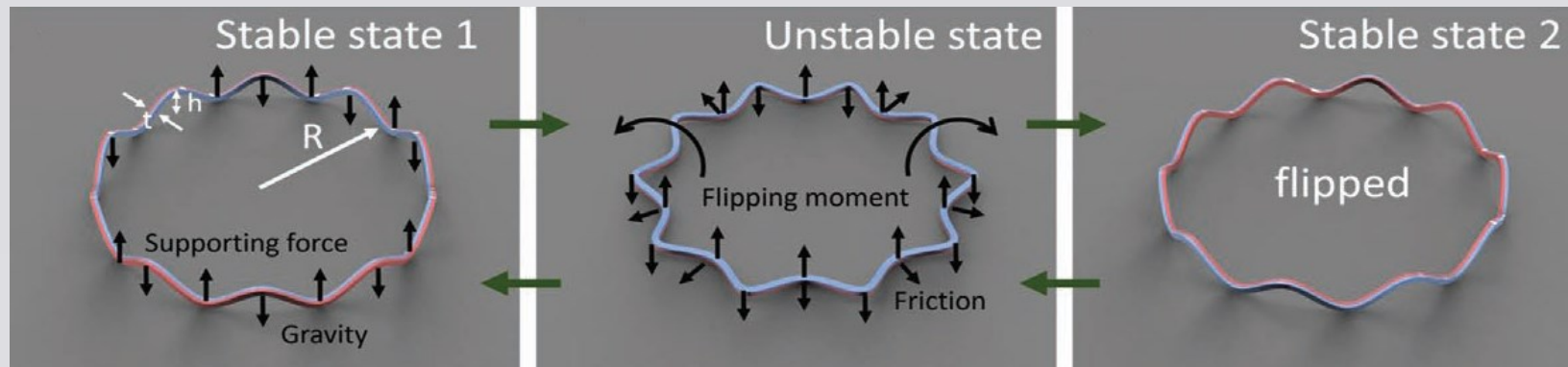
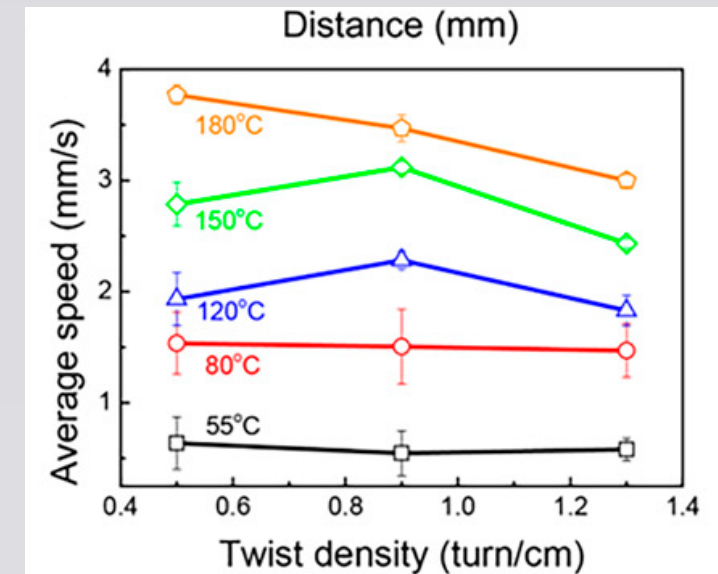


Figure 4: Snapping process in the wavy rings

LCE Twisting Robots Dynamics[1]

- The average rolling speed of the twisted ribbons is mainly determined by the temperature of the hot surfaces they roll on. Higher twist density defined as the number of twists per unit length results in more contact points, but not necessarily higher average rolling speeds.

Figure 5:
Average
rolling speed
based on
temperature
and twist
density



LCE Twisting Robots Dynamics[1]

- After the twisted ribbons reach thermodynamic equilibrium, both of its ends spin at the same angular velocity and its twist density remains constant
- Locomotion on granular surfaces is more challenging and therefore slower than locomotion on hard flat surfaces.

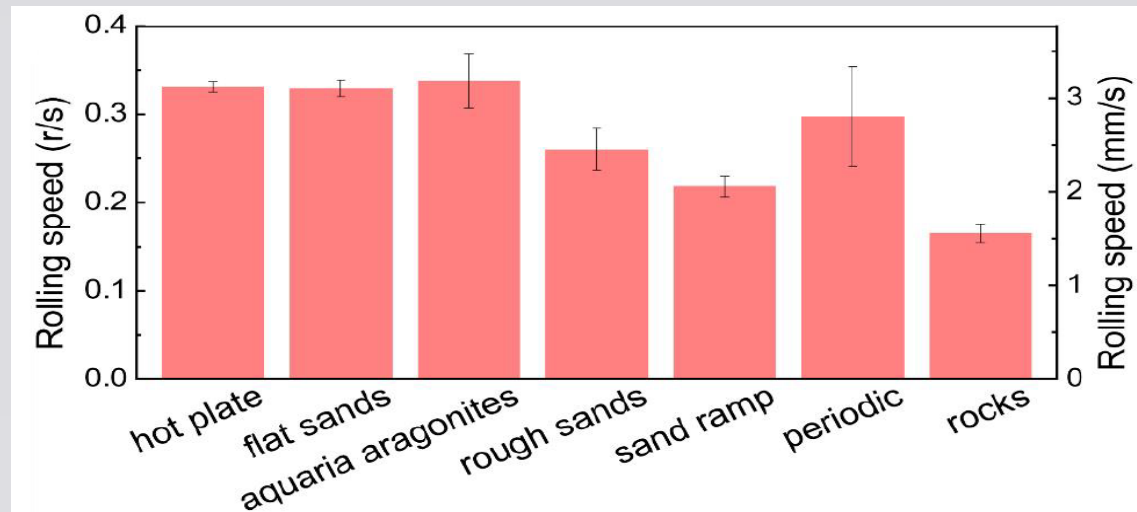


Figure 6: Rolling speed of twisting ribbon robots on different surfaces

Ribbon Geometry[5]

- A ribbon surface S in with length l and width w can be described by its centerline curve r :

$M, = (d_1 d_2, d_3)$: Frenet frame

$\kappa = d_3' \cdot d_1$: Curvature

$\tau = d_1' \cdot d_2$: torsion $d_2' \cdot d_3 = 0$

$$\begin{aligned}
 S(u, v) &= \mathbf{r}(u) + v\boldsymbol{\omega}(u) , \\
 \boldsymbol{\omega}(u) &= d_2(u) + \eta(u) d_3(u) , \\
 \eta(u) &= \tau(u)/\kappa(u) \\
 u &\in [0, l], v \in [-\omega/2, \omega/2].
 \end{aligned}$$

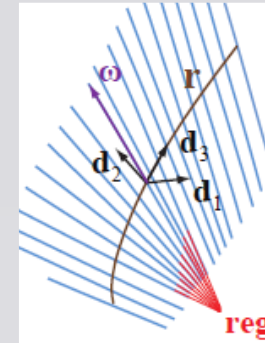


Figure 7: The ribbon surface

- A highly efficient simulation method has two steps for each iteration. The first step is solving the dynamic equation for the centerline and in the second step, the new geometry of the ribbon is constituted from the new position of the centerline and the constraints of the system

Ribbon Geometry[1]

- Unlike twisted ribbons, helical ribbons are incapable of self rolling by harnessing thermal energy from the environment.

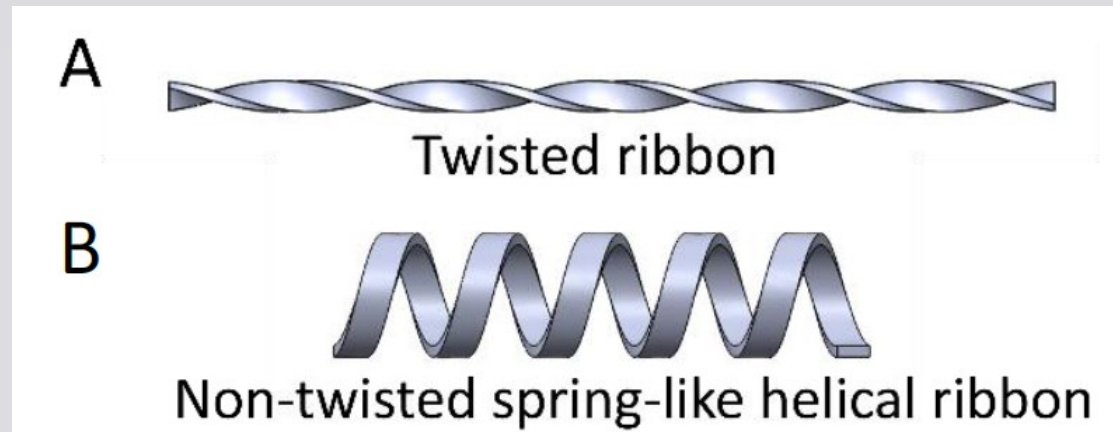


Figure 8: Twisted and helical ribbons



Contact Model[6],[7]

- Having an implicit contact model instead of the usual ones based on explicit constraints makes computations much faster.
- Contact can be modeled by adding a contact energy to the system. This energy function should be smooth to make computations based on Newton-Raphson method reliable.
- Allowing small penetrations makes computations faster and prevents jittering
- The model for friction is the simple Coulomb's law

Contact Model- Contact Energy [6],[7]

- One candidate for the contact energy function is:

$$E(\Delta, \delta) = \begin{cases} (2h - \Delta)^2 & \Delta \in (0, 2h - \delta] \\ \left(\frac{1}{K_1} \log(1 + \exp(K_1(2h - \Delta)))\right)^2 & \Delta \in (2h - \delta, 2h + \delta) \\ 0 & \Delta \geq 2h + \delta, \end{cases}$$

$2h$: Minimum distance of contact force engagement $K_1 = 15/\delta$

Δ : The distance between two surfaces δ : Parameter that smoothes the function

Contact Model- Kinetic Friction [6],[7]

$$\mathbf{F}^c \equiv k\nabla_{\mathbf{x}} E$$

$$\mathbf{n}_i = \frac{\mathbf{F}_i^c + \mathbf{F}_{i+1}^c}{\|\mathbf{F}_i^c + \mathbf{F}_{i+1}^c\|}$$

$$\mathbf{v}_i^e = (1 - \beta_i)\mathbf{v}_i + \beta_i\mathbf{v}_{i+1},$$

$$\mathbf{v}_j^e = (1 - \beta_j)\mathbf{v}_j + \beta_j\mathbf{v}_{j+1},$$

$$\mathbf{v}^{\text{rel}} = \mathbf{v}_i^e - \mathbf{v}_j^e,$$

$$\mathbf{v}^{\text{Trel}} = \mathbf{v}^{\text{rel}} - (\mathbf{v}^{\text{rel}} \cdot \mathbf{n}_i)\mathbf{n}_i,$$

$$\hat{\mathbf{v}}^{\text{Trel}} = \mathbf{v}^{\text{Trel}} / \|\mathbf{v}^{\text{Trel}}\|$$

$$F_i^n = \|\dot{\mathbf{F}}_i^c\|$$

$$\beta = \frac{\|\mathbf{F}_{i+1}^c\|}{\|\mathbf{F}_i^c + \mathbf{F}_{i+1}^c\|}$$

F^c : Contact force (normal) n_i : i-th contact norm vector v_i : velocity of the i-th node

v^{rel} : relative velocity of i-th and j-th node v^{Trel} : Tangential component of v^{rel}

\hat{v}^{Trel} : Direction of v^{Trel}

Contact Model- Static Friction [6]

- The transition between static and kinetic friction should also be smooth.

$$\gamma(\|\mathbf{v}^{\text{Trel}}\|, \nu) = \frac{2}{1 + \exp(-K_2\|\mathbf{v}^{\text{Trel}}\|)} - 1, \quad K_2(\nu) = 15/\nu \quad \mathbf{F}_i^{\text{fr}} = -\mu\gamma\hat{\mathbf{v}}^{\text{Trel}}F_i^n.$$

ν : Desired slipping tolerance μ : Friction coefficient

F_i^{fr} : Friction force at node i of the contact pair of i and j

Contact Model [6]

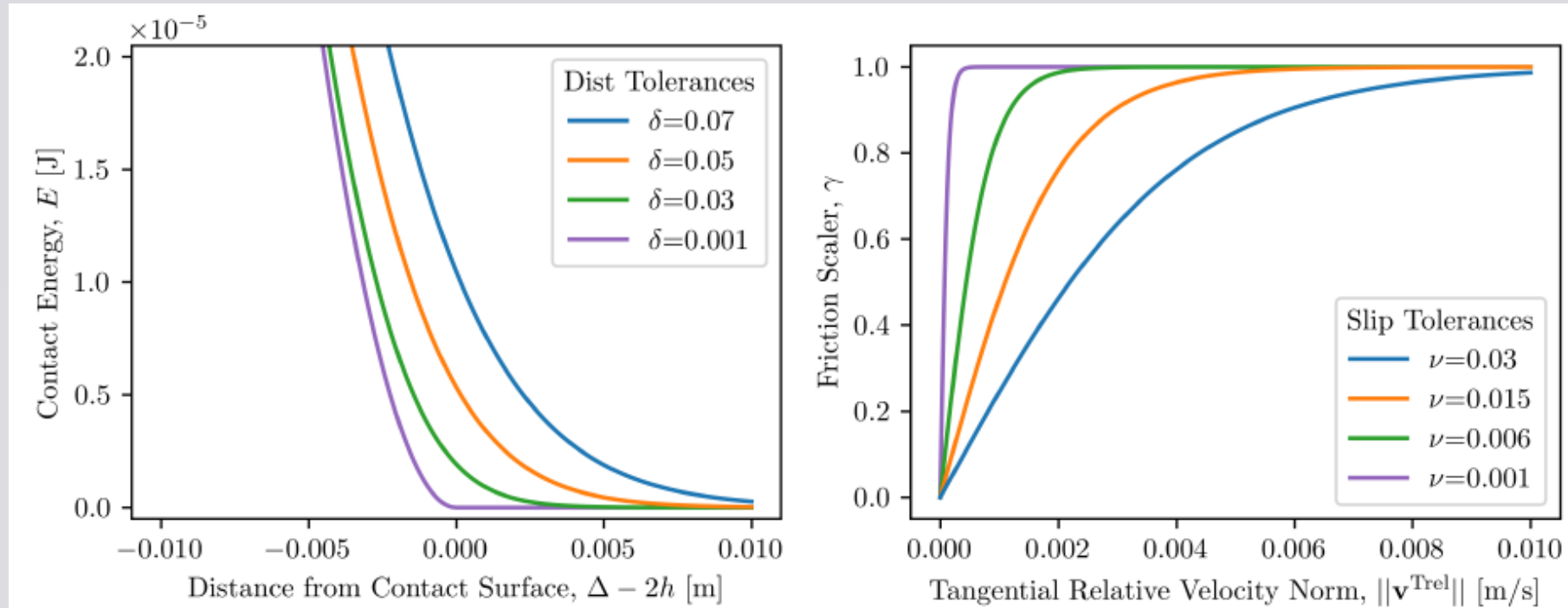


Figure 9: Graphs of contact energy based on distance (left) and friction force based on relative tangential speed (right)



Discrete Elastic Rods (DER) [8]

- DER is a powerful computational framework for simulation and design of soft robots
- DER can capture important elements of system dynamics such as contacts and inertial effects.
- DER is highly accurate and agrees with experimental results and is computationally efficient enough to be used in real time.

DER- Parallel Transport [8],[9],[10],[11],[12]

- $P_{k-1}^k = \text{parallel transport}(u, t^{k-1}, t^k) = d$
- Parallel transport can be done to the next edges either in time or in space.

The difference between the signed angle of

Two consecutive edges i and $i+1$ from the parallel transports of a common edge is called integrated twist τ_i

$$\mathbf{b} = \mathbf{t}^{k-1} \times \mathbf{t}^k,$$

$$\hat{\mathbf{b}} = \frac{\mathbf{b}}{|\mathbf{b}|},$$

$$\mathbf{n}_1 = \mathbf{t}^{k-1} \times \hat{\mathbf{b}},$$

$$\mathbf{n}_2 = \mathbf{t}^k \times \hat{\mathbf{b}},$$

$$\mathbf{d} = (\mathbf{u} \cdot \mathbf{t}^{k-1})\mathbf{t}^k + (\mathbf{u} \cdot \mathbf{n}_1)\mathbf{n}_2 + (\mathbf{u} \cdot \hat{\mathbf{b}})\hat{\mathbf{b}}.$$

DER- Parallel Transport[9]

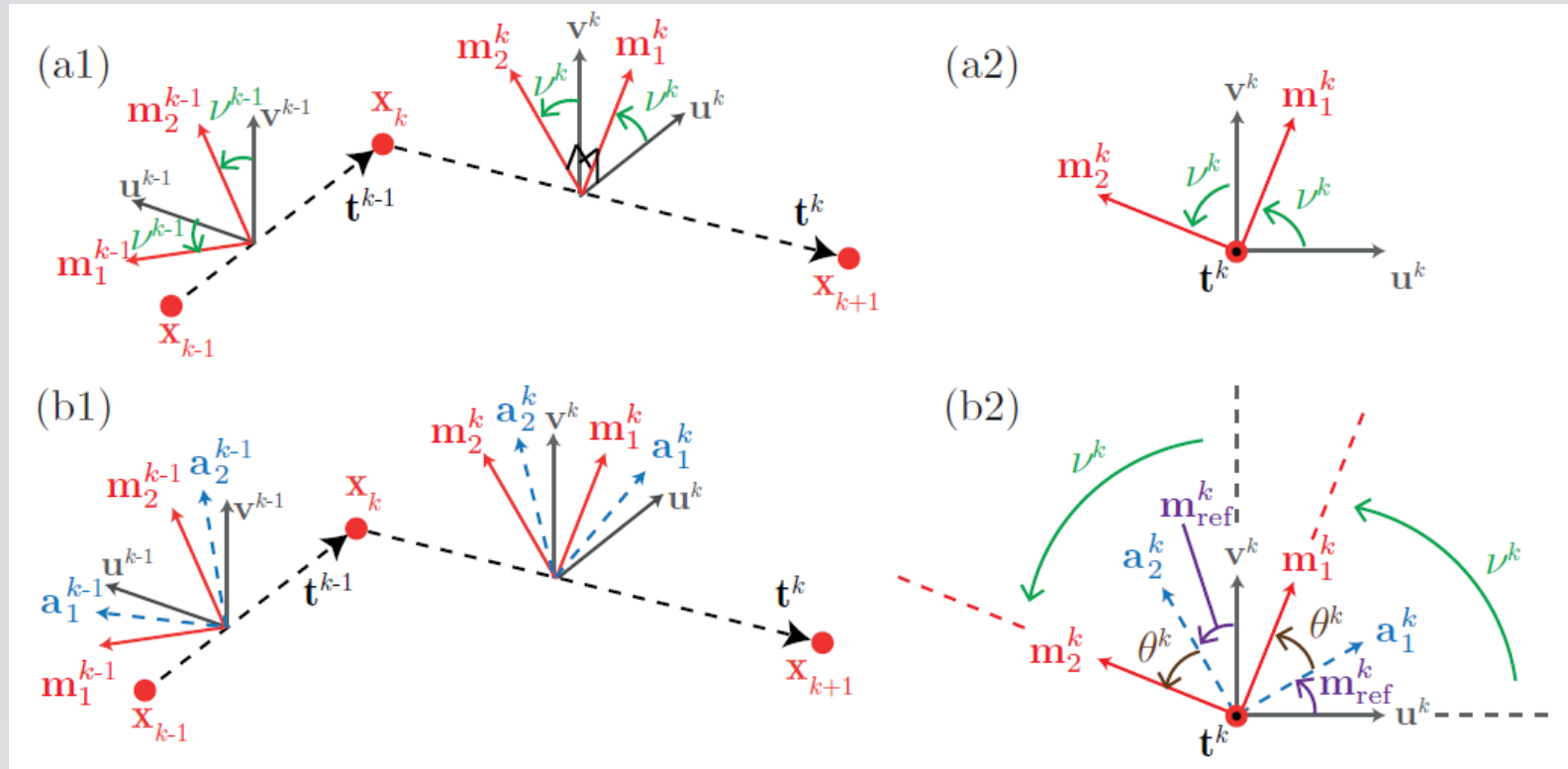


Figure 10: Parallel transport

DER- Energy Components [8],[9],[10],[11],[12]

- Stretching energy:

$$E_k^s = \frac{1}{2}EA \left(\frac{|\mathbf{x}_{k+1} - \mathbf{x}_k|}{|\bar{\mathbf{e}}^k|} - 1 \right)^2 |\bar{\mathbf{e}}^k|,$$

$$\mathbf{e}^k = \mathbf{x}_{k+1} - \mathbf{x}_k$$

$$\mathbf{t}^k = \frac{\mathbf{e}^k}{|\mathbf{e}^k|}$$

- Bending Energy:

$$E_k^b = \frac{1}{2}EI \left(|\boldsymbol{\kappa}_k - \boldsymbol{\kappa}_k^0| \right)^2 \frac{1}{\bar{l}_k},$$

$$\bar{l}_k = (|\mathbf{e}^{k-1}| + |\mathbf{e}^k|) / 2$$

- Twisting Energy:

$$E_k^t = \frac{1}{2}GJ\tau_k^2 \frac{1}{\bar{l}_k},$$

$$I = \pi r_0^4 / 4$$

$$J = \pi r_0^4 / 2.$$

$$(\kappa b)_k = \frac{2\mathbf{t}^{k-1} \times \mathbf{t}^k}{1 + \mathbf{t}^{k-1} \cdot \mathbf{t}^k},$$

$$\kappa_1 = \frac{1}{2}(\kappa b)_k \cdot (\mathbf{m}_2^{k-1} + \mathbf{m}_2^k),$$

$$\kappa_2 = -\frac{1}{2}(\kappa b)_k \cdot (\mathbf{m}_1^{k-1} + \mathbf{m}_1^k),$$

$$\boldsymbol{\kappa}_k = [\kappa_1, \kappa_2],$$

$$E_{\text{elastic}} = \underbrace{\sum_{k=1}^{N-1} E_k^s}_{\text{stretching energy}} + \underbrace{\sum_{k=2}^{N-1} E_k^b}_{\text{bending energy}} + \underbrace{\sum_{k=2}^{N-1} E_k^t}_{\text{twisting energy}},$$

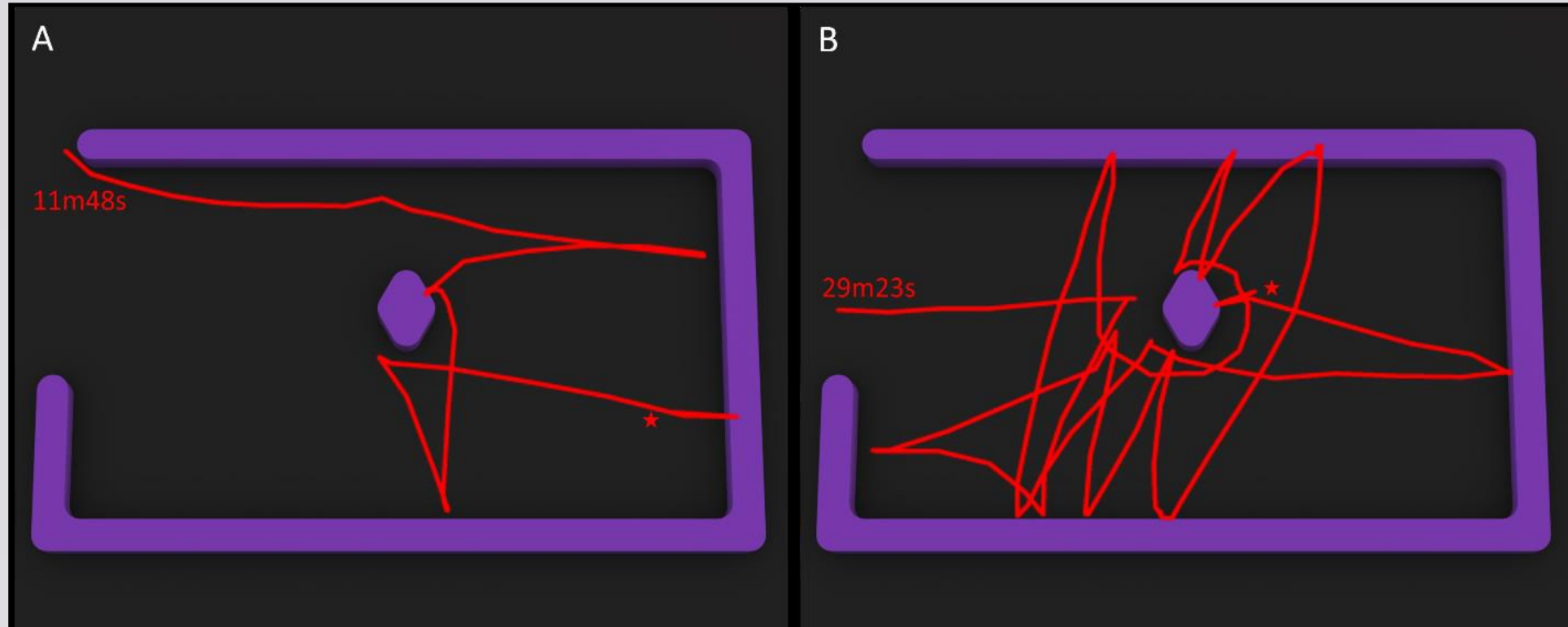
X_k : k - th node
 e_k : k - th edge

DER Differential Equation [8],[9],[10],[11],[12]

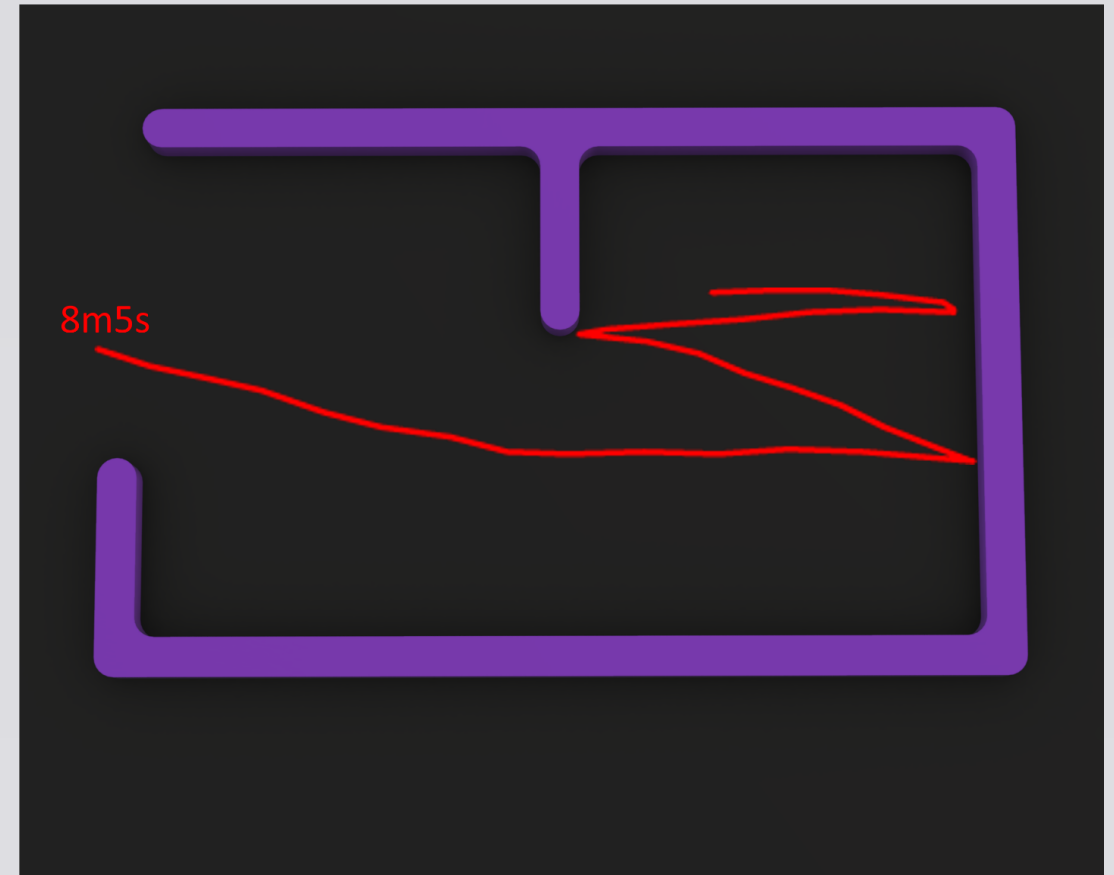
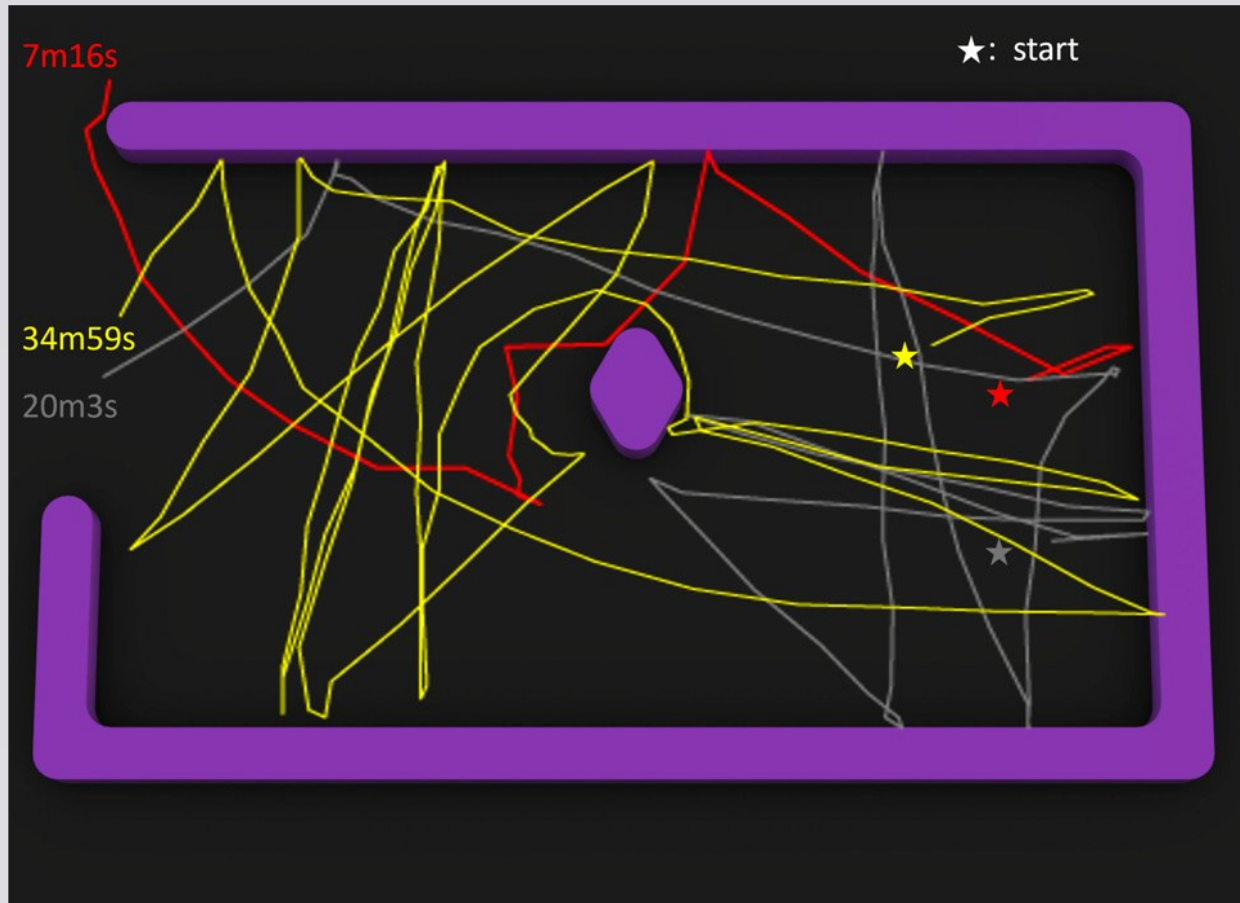
- The equations are usually solved implicitly by Newton-Raphson method.
- Most common external forces are gravity, contact and friction forces and Viscous damping

$$f_i \equiv \frac{m_i}{\Delta t} \left[\frac{q_i(t_{j+1}) - q_i(t_j)}{\Delta t} - \dot{q}_i(t_j) \right] + \frac{\partial E_{\text{elastic}}}{\partial q_i} - f_i^{\text{ext}} = 0,$$

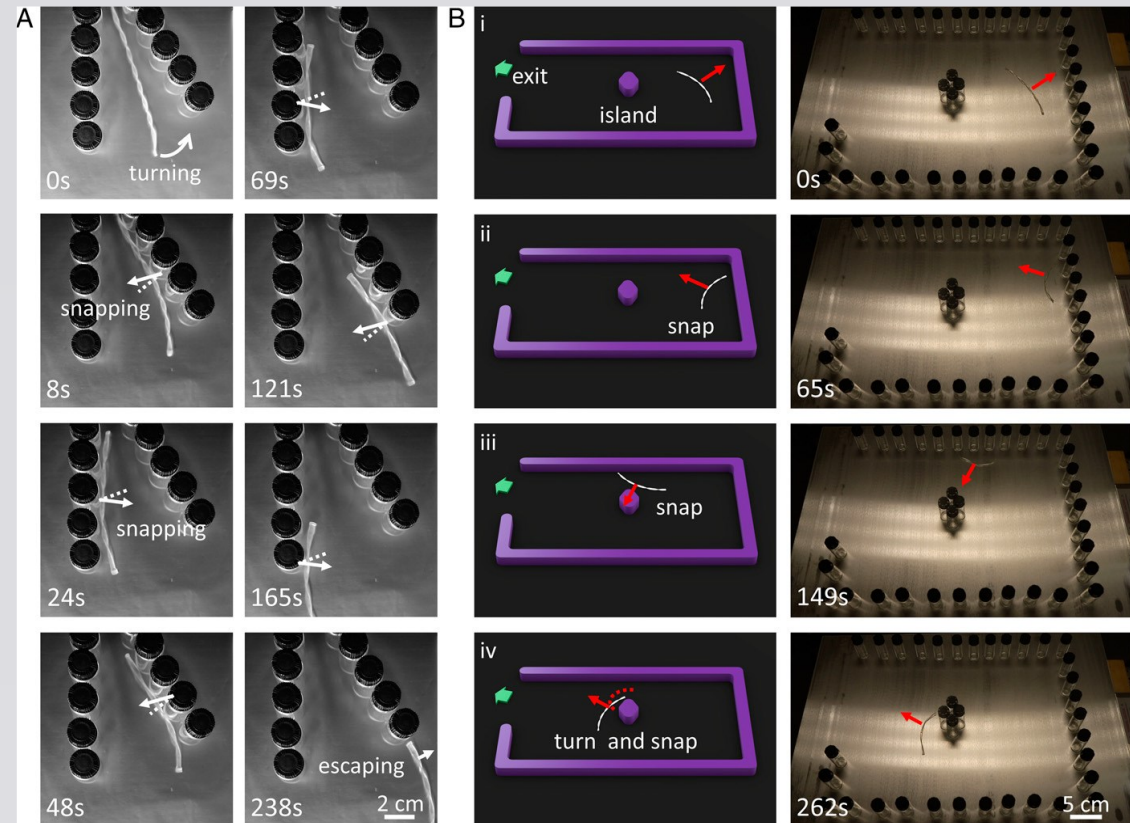
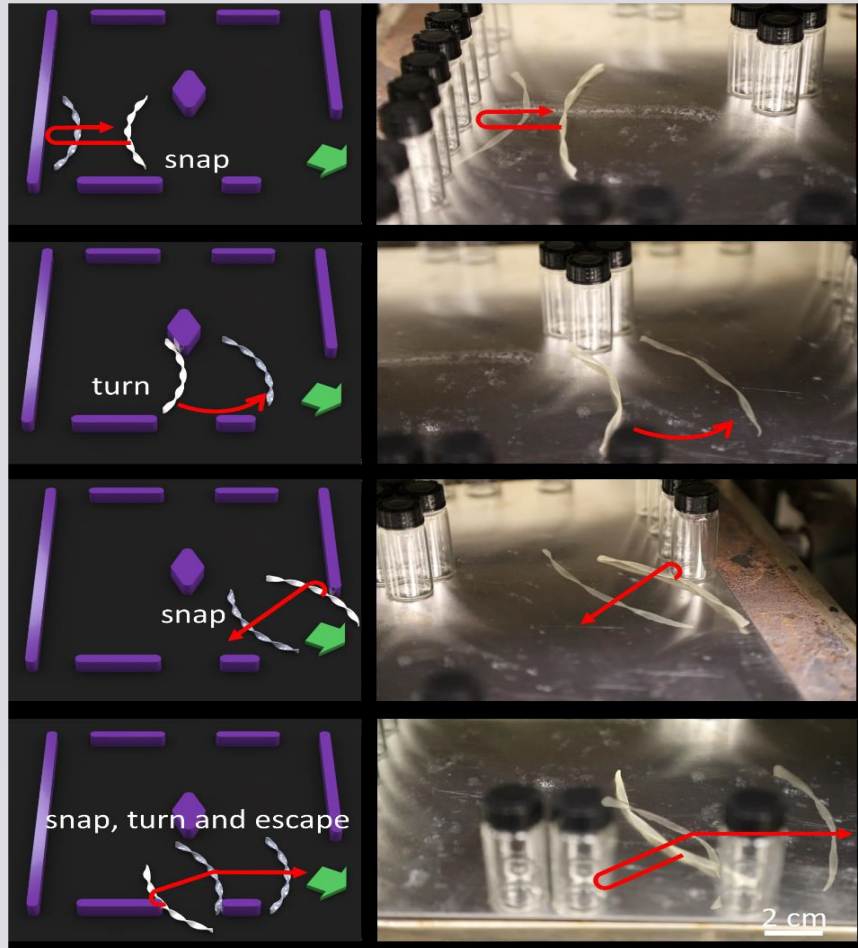
Interesting Case of Escaping from Mazes[1]



Interesting Case of Escaping from Mazes[1]



Interesting Case of Escaping from Mazes[1]





References

- 1- “Twisting for soft intelligent autonomous robot in unstructured environments” written by Yao Zhao, Yinding Chia, Yaoye Hong, Yanbin Lia, Shu Yangb and Jie Yina _ PNAS 2022
- 2- “Liquid Crystal Elastomer Actuators: Synthesis, Alignment, and Applications” written by Ruvini S. Kularatne, Hyun Kim, Jennifer M. Boothby, Taylor H. Ware _ Journal of Polymer Science-Polymer Physics 2016
- 3- “Self-Sustained Snapping Drives Autonomous Dancing and Motion in Free-Standing Wavy Rings” written by Yao Zhao, Yaoye Hong, Fangjie Qi, Yinding Chi, Hao Su, and Jie Yin _ Advanced Materials 2022
- 4-” Statistical Mechanics of Developable Ribbons” written by L. Giomi and L. Mahadevan _ Physical Review Letters 2010



References

- 5- “Geometrically Exact Simulation of Inextensible Ribbon” written by Zhongwei Shen, Jin Huang, Wei Chen and Hujun Bao _ Pacific Graphics 2015
- 6-” A Fully Implicit Method for Robust Frictional Contact Handling in Elastic Rods” written by Dezhong Tong, Andrew Choi, Jungseock Jooc, M. Khalid Jawed _ Elsevier 2022
- 7- “Implicit Contact Model for Discrete Elastic Rods in Knot Tying” written by Andrew Choi, Dezhong Tong, Mohammad K. Jawed and Jungseock Joo _ Journal of Applied Mechanics 2021
- 8- “Dynamic simulation of articulated soft robots” written by Weicheng Huang, Xiaonan Huang, Carmel Majidi and M. Khalid Jawed _ Nature Communication 2020



References

- 9- “Notes on Discrete Simulation of Slender Structures” written by Khalid Jawed _ UCLA 2020
- 10- “A Primer on the Kinematics of Discrete Elastic Rods” written by M. Khalid Jawed, Alyssa Novelia and Oliver M. O’Reilly _ Springer 2018
- 11- “Discrete Elastic Rods” Written by Miklos Bergou, Max Wardetzky, Stephen Robinson, Basile Audoly and Eitan Grinspun _ Columbia University 2008
- 12- “Numerical Simulation of an Untethered Omni-Directional Star-Shaped Swimming Robot”
Written by Xiaonan Huang, Weicheng Huang, Zachary Patterson, Zhijian Ren, M. Khalid Jawed and Carmel Majidi _ IEEE International Conference on Robotics and Automation 2021